Vietnam Journal of Mechanics, Vol. 45, No. 3 (2023), pp. 235 – 246
DOI: https://doi.org/10.15625/0866-7136/19023

# MICROMECHANICAL MODEL TO PREDICT THE EFFECT OF TEMPERATURE ON THE BEHAVIOR OF UNSATURATED POROUS MEDIA

**Bao Viet Tran**[1,*], **Xavier Chateau**[2]
[1]*Construction Engineering Faculty, Research and Application Center for Technology in Civil Engineering, University of Transport and Communications, Lang Thuong, Dong Da, Hanoi, Vietnam*
[2]*Navier, Ecole des Ponts, Univ Gustave Eiffel, CNRS, Marne-la-Vallée, France*
[*]E-mail: viettb@utc.edu.vn

Received: 11 September 2023 / Published online: 30 September 2023

**Abstract.** The homogenization method is used to investigate temperature effects on the water content–capillary pressure relationship and on the poro–mechanical behavior of unsaturated porous media. Two different phenomena have been considered: the temperature variations of surface tensions and the thermal dilatation of the solid phase in the framework of micromechanical models that are proposed in order to highlight the influence of the deformability of the solid phase on the macroscopic behavior. The result show that taking into account the coupling between the deformation of the porous space and the capillary effects can radically modify the prediction of the temperature influence on the capillary curve.

*Keywords*: beam, nonlinear vibration, vibration equation, resonance oscillation, asymptotic method.

## 1. INTRODUCTION

The influence of temperature on the properties of geomaterials is of major concern in the design of engineering applications as high-level radioactive waste disposal [1]. To relate the effects of partial saturation and temperature changes within a macroscopic thermodynamic framework requires one is able to postulate the form of macroscopic constitutive laws from experimental data. Because of couplings between many phases and of the experimental evidence that most of the unsaturated porous media have a non linear behavior, this question is still debated. For instance, such an important question as the temperature effects on the water content–capillary pressure relationship has not yet

received a satisfactory answer. Because of its ability to incorporate at the macroscopic level the physics of the microscopic level as well as the morphological aspects, at least partly, it is believed that homogenization methods may be a helpful modeling tool. In the present paper, the formulation of the thermo–poro–mechanical behavior of unsaturated media is addressed within the framework of upscaling techniques.

In the first section following the introduction, it is briefly recalled that the water content-capillary pressure curve scales like the surface tension in the capillary interface when it is assumed that the solid matrix is rigid and the interactions between the solid phase and the capillary interfaces are described by the classical Laplace and Young-Dupré laws [2]. Then, departure from this scaling law may be ascribed to deformation of the solid phase or to physico chemical interactions between the fluid phases and the solid matrix. In this paper, only the effects of solid phase deformations are taken into account.

In order to evaluate the influence of the solid phase deformability, we address the situation where the solid matrix is linear elastic.

In the third section of this paper, the porous space is modeled as a set of spherical pores which are either filled by liquid or by gas. Special attention is devoted to the link between the sorption-desorption hysteretic phenomena and the thermo-mechanical behavior of the porous medium. In the fourth section of the paper, we consider the situation where the porous space is made up of cracks connected one another. Unlike the previous model, this model accounts for nonlinear coupling between the solid matrix strains and the capillary internal forces. It is shown that this coupling induces temperature effects on the water content–capillary pressure relationship. A brief conclusion is given at the end of the paper.

## 2. RIGID POROUS MATERIALS

To begin with, it is assumed that the solid phase is made up of a rigid material. In this situation, the water content–capillary pressure relationship depends on the morphological properties of the porous space and on the surface tension values. Then, the temperature variations of the surface tensions are expected to induce change of the water content–capillary pressure relationship. The main problem one has to face to model the temperature effects on the water retention curve of porous media is the lack of experimental data. Whereas it is rather difficult to experimentally measure the solid–fluid surface tension on well–defined samples [3], it is even more difficult, if not impossible, to estimate these quantities for porous materials. In most of the situations of practical interest, only the relationship between the liquid–gas surface tension and the temperature is known. Consequently, it is generally assumed that the wetting angle does not depend on the temperature.

Let us consider a rigid porous material, the porous space of which is filled by a liquid and a gas. For simplicity, it is assumed that the liquid perfectly wets the solid phase and the solid–liquid surface tension is naught. Then the surface tension in the liquid-gas interface and in the solid-gas interface are equal. Temperature dependence of surface tensions is described by the law:

$$\gamma(\theta) = \gamma_0 f(\theta), \tag{1}$$

where $\theta$ denotes the temperature difference between the current configuration and the reference configuration, $\gamma(\theta)$ the solid–gas and the liquid–gas surface tensions at temperature $\theta$ and $\gamma_0$ is the surface tension at the reference temperature. When the unsaturated material is in mechanical and thermodynamical equilibrium at temperature $\theta$, the pressures are uniform over the domains occupied by the fluid phases, even if these domains are not connected. The fluid pressures are then related by the Laplace law

$$p_c(\theta) = p_g(\theta) - p_\ell(\theta) = \frac{2\gamma(\theta)}{r_{\ell g}}, \tag{2}$$

where $2/r_{\ell g}$ denotes the mean curvature of the liquid–gas interface. Putting Eq. (1) into Eq. (2) yields the relationship between the capillary pressure and the temperature for a given configuration of the capillary interface within the porous space:

$$p_c(\theta) = \frac{\gamma(\theta)}{\gamma_0} p_c(0). \tag{3}$$

Then, it is easily seen from Eq. (3) that when all the assumptions described above are fulfilled, the water content–capillary pressure relationship is described by a master curve as depicted in Fig. 1.

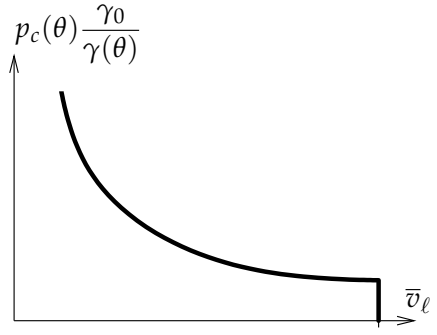


*Fig. 1.* Water retention master curve for a rigid porous medium in the normalized water content–normalized capillary pressure diagram

Interestingly, this property does not depend on the morphology of the studied porous medium.

## 3. LINEAR POROELASTIC MODEL

The thermo–poro–elastic behavior of an unsaturated porous medium is addressed in the framework of upscaling techniques performing exactly the same approach that in [4] the only difference coming from the temperature changes considered in this paper. The mechanical loading applied to the representative elementary volume of porous medium is now defined by the macroscopic strain $\boldsymbol{E}$ and by the temperature $\theta$. At the microscopic level, the solid obeys the state law

$$\boldsymbol{\sigma} = \mathbb{C} : (\boldsymbol{e} - \boldsymbol{\alpha}\theta). \tag{4}$$

where $\mathbb{C}$ denotes the isothermal tensor of elastic moduli of the solid phase while $\boldsymbol{\alpha}$ is the thermal expansion tensor of the solid phase. Both quantities are assumed to be uniform over the solid domain (homogeneous solid phase). The internal forces in the porous space are described by the liquid pressure $p_\ell$ in the liquid domain, the gas pressure $p_g$ in the gaseous domain and by the surface tension $\gamma(\theta)$ in the gas–liquid and the solid–gas interfaces (it is again assumed that the liquid phase perfectly wets the solid phase and that the surface tension is naught in the liquid–solid interface). It is also assumed that the porous space is made up of $N$ subsets of spherical pores, each subset being characterized by the pore radius $R_\beta$ and the volume fraction $S_\beta$ ($\beta = 1, \ldots, N$). The distribution of liquid and gas in the pore network is described by the set $I_g$ according to the following rule: if $\beta \in I_g$, the pores of the subset $\beta$ are filled with gas whereas they are filled with liquid if $\beta \notin I_g$. Then, performing exactly the same computations that in [4], it is shown that the general formulation of the macroscopic state law is

$$\begin{aligned} \boldsymbol{\Sigma} = \mathbb{C}_h : (\boldsymbol{E} - \boldsymbol{\alpha}\theta) + \left(S_r p_c - p_g\right) \boldsymbol{B} \\ + \sum_{\beta \in I_g} \frac{2\gamma(\theta)}{R_\beta} S_\beta \boldsymbol{B}, \end{aligned} \tag{5}$$

where $\mathbb{C}_h$ denotes the overall elastic tensor, $\boldsymbol{B}$, the Biot tensor and $S_r$ the saturation ratio. It is recalled that the Biot tensor reads

$$\boldsymbol{B} = \boldsymbol{\delta} : \left(\mathbb{I} - \mathbb{C}^{-1} : \mathbb{C}_h\right), \tag{6}$$

where $\boldsymbol{\delta}$ denotes the second order unit tensor and $\mathbb{I}$ the fourth order unit tensor.

In order to relate the evolutions of the set $I_g$ to the variations of the capillary pressure, we use the classical model in which the pore network is made up of spherical pores of decreasing radius connecting one another by capillary necks of decreasing radius $r_\beta$ as described in [4,5] (see Fig. 2).

As it is well known, this model explains the hysteresis of the capillary curve by the fact that the capillary pressure at which the gas enters the pore is controlled by the neck radius $r_\beta$ whereas the liquid enters the pore at a capillary pressure controlled by the pore

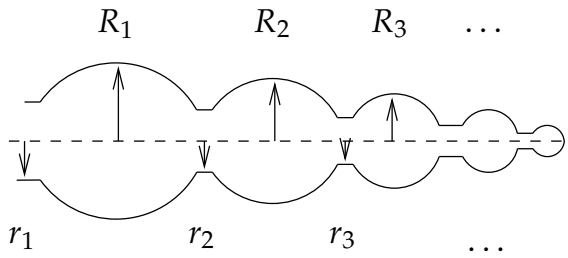


*Fig. 2.* A morphological model for the hysteresis of the capillary curve

radius $R_\beta$. In the framework of this sample model, the overall state law reads

$$\begin{aligned}\boldsymbol{\Sigma} = \mathbb{C}_h : (\boldsymbol{E} - \boldsymbol{\alpha}\theta) \\ + \left(S_r p_c - p_g + \Sigma_g(S_r, \theta)\right) \boldsymbol{B},\end{aligned} \tag{7}$$

with $\Sigma_g(S_r, \theta)$ defined by (see Fig. 3):

$$\Sigma_g(S_r, \theta) = \int_{S_r}^{1} p_c(\theta)(dSr > 0) dS_r. \tag{8}$$

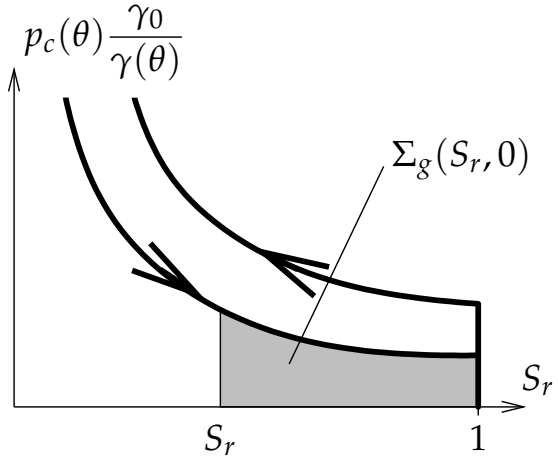


*Fig. 3.* Prestress $\Sigma(S_r, 0)$ in the capillary pressure–saturation ratio diagram

In Eq. (8), $p_c(\theta)(dSr > 0)$ denotes the imbibition saturation–capillary pressure relationship. As the saturation ratio–capillary pressure relationship is evaluated on the unloaded configuration at $\theta = 0$, the water retention behavior of the material is again described by a master curve in the water content–normalized capillary pressure diagram. Then, this micromechanical model does not explain why some materials do not obey the simple rule depicted in Fig. 1. Nevertheless, this micromechanical model accounts for temperature effects on the poromechanical behavior of the porous medium as a function

of both the thermal dilatation of the solid phase and the temperature variations of surface tension. As the unsaturated porous state law reads:

$$\begin{aligned}\boldsymbol{\Sigma} = \mathbb{C}_h : (\boldsymbol{E} - \boldsymbol{\alpha}\theta) \\ + \frac{\gamma(\theta)}{\gamma_0}\left(S_r p_c(0) - p_g + \Sigma_g(S_r, 0)\right)\boldsymbol{B},\end{aligned} \tag{9}$$

it can be evaluated from the knowledge of the water content–capillary pressure diagram measured at the reference temperature, the thermal dilatation tensor of the solid matrix $\boldsymbol{\alpha}$ and the drained mechanical tensors $\mathbb{C}_h$ and $\boldsymbol{B}$. State Eq. (9) generalizes the model described in [2] to the situations in which temperature effects can not be neglected. As for the isothermal evolutions of the system, the capillary pressure curves and the drained thermo–mechanical properties allow to characterize the thermo–mechanical behavior in unsaturated conditions.

## 4. NONLINEAR POROELASTIC MODEL

We now take into consideration the coupling between the deformation of the pores and the capillary effects. We consider an unsaturated mesocracked medium the pores of which are modeled as oblate ellipsoids as described in [6,7] (see Fig. 4).

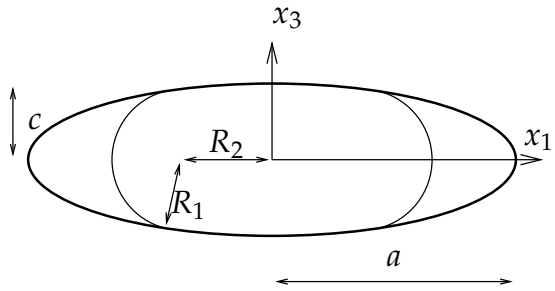


*Fig. 4.* The unsaturated elliptic crack

For simplicity, we only consider the situations where the cracks are identical (ie same shape, same size and same capillary state) except for theirs orientations. More precisely, it is assumed that each crack can be satisfactory described by an oblate ellipsoid with radius $a$ and opening $c$ (see Fig. 4). The dilute scheme, pertinent to the situations where one can consider that the cracks are not interacting, is adopted. Furthermore, it is assumed that the cracks are isotropically distributed within an isotropic solid matrix. It is convenient to introduce the aspect ratio $X = c/a$ and the crack density $\varepsilon$ defined by $n = 4/3\pi$ [8]. $n$ denotes the porosity in the actual configuration. The overall behavior of the material is isotropic characterized in the dry situation by the shear modulus $\mu_h$

$$\mu_h = \mu\,(1 - \beta)\,, \tag{10}$$

with

$$\beta = \frac{32}{45}\varepsilon\frac{(5-\nu)(1-\nu)}{2-\nu}, \tag{11}$$

and the bulk modulus $k_h$

$$k_h = k\,(1-b) \quad \text{with} \quad b = \frac{16}{9}\varepsilon\frac{1-\nu^2}{1-2\nu}, \tag{12}$$

where $\mu$ and $k$ denote the shear modulus and the bulk modulus of the solid matrix and $\nu$ is the Poisson ratio. It is worth noting that the elastic properties of the cracked medium does not depend on the aspect ratio of the cracks [6,7]. Then the macroscopic state equation is linear in the saturated regime as long as the cracks remain open.

When thermal expansion of the solid phase and temperature variation of the surface tensions are taken into account, the overall behavior of the unsaturated cracked material is obtained performing exactly the same approach that in [6]. The macroscopic thermal expansion tensor of the cracked material is equal to that of the solid matrix.

When the cracks are saturated by a fluid at pressure $p$, the change of scale approach allows to recover the classical Biot state law of poroelasticity [9]

$$\boldsymbol{\Sigma} + pb\boldsymbol{\delta} = \mathbf{C}_h : (\boldsymbol{E} - \alpha\theta\boldsymbol{\delta}). \tag{13}$$

To address the unsaturated regime, it is assumed that the distribution of the fluid phases inside the cracks complies with the property of cylindrical symmetry around the smaller axis of the crack. The solution of this problem is carried out within the framework of the toroidal approximation [10,11]. The intersection of the liquid–gas interface with a plane containing the small axis of the ellipsoid is approximated by an arc of a circle with radius $R_1$, whose center is located in the plane $Ox_1x_3$ at a distance $R_2$ from the axis $0x_3$ (Figure 4). Within the framework defined by this approximation, it is possible to compute analytically both the capillary pressure and the the average of the capillary forces with consideration of the presence of the fluids in the pore.

Using the approximation $X \ll 1$ into the equations allowing to compute the capillary pressure and the saturation ratio yields the following equation for the capillary curve

$$p_c = \frac{\gamma}{aX}\frac{1}{\cos\varphi}, \qquad S_r = \cos^3\varphi, \tag{14}$$

where $\varphi$ is a scalar varying from 0 to $\pi/2$. The average of the prestress (defined as the fluid pressure in the fluid domains and the surface tension in the interfaces) over the domain occupied by a crack reads

$$< \boldsymbol{\sigma}_p >= \frac{\gamma}{aX}\left(\frac{3-cos^2\varphi}{2}\boldsymbol{\delta} - \frac{3}{2}\sin^2\varphi\,\underline{e}_3\otimes\underline{e}_3\right) - p_g\boldsymbol{\delta}. \tag{15}$$

The quantity $(\underline{e}_3 \otimes \underline{e}_3) :< \boldsymbol{\sigma}_p >$ is denoted by $\sigma_p$ in the sequel. It is easily shown from Eq. (15) that we have

$$\sigma_p = \frac{\gamma \cos^2 \varphi}{aX} - p_g = \frac{\gamma^3}{a^3 X^3} \frac{1}{p_c^2} - p_g. \tag{16}$$

Of course, the surface tension $\gamma$ involved in Eqs. (14), (15) and (16) depends upon the temperature $\theta$.

We now investigate the effect of the variation of the cracks aspect ratio on the overall behavior of the unsaturated cracked material. The possibility of a total closing of cracks is set aside. Due to the geometrical change, an incremental approach is necessary.

When the free stress configuration is taken as a reference, it can be shown that the overall state law reads

$$\boldsymbol{\Sigma} = \mathbb{C}_h : (\boldsymbol{E} - \alpha\theta\boldsymbol{\delta}) + \boldsymbol{\Sigma}_p, \tag{17}$$

with

$$\boldsymbol{\Sigma}_p = \varepsilon \int_{\varphi=0}^{\varphi=\pi} \int_{\psi=0}^{\psi=2\pi} \frac{X < \boldsymbol{\sigma}_p >}{3} \mathbb{T} \sin\varphi d\psi d\varphi. \tag{18}$$

The macroscopic prestress $\boldsymbol{\Sigma}_p$ is computed by integrating the microscopic quantities over the definition set for Euler's angles. In Eq. (18), the quantities $X$, $\mathbb{T}$ and $< \boldsymbol{\sigma}_p >$ usually depend on the Euler's angles. For each crack, $\mathbb{T}(\psi, \varphi)$ is a fourth order tensor allowing to compute the deformation of the crack as a function of the macroscopic prescribed strain in the isothermal dry regime [7].

Strictly speaking, Eq. (17) is valid only if the cracks shape remains that of an oblate ellipsoid in the course of the material deformation. As this property holds only if the prestress tensor is uniform over the cracks domain, the state law (17) may be seen as a first estimate to the behavior of unsaturated cracked materials accounting for the cracks geometry change. Similarly, it is assumed in the sequel that the results allowing to compute the average of the prestress tensor over the cracks are still valid when the cracks deform.

The localization tensor $\mathbb{T}$ relates the cracks strain increment to the increment of the macroscopic strain and the variation of the prestress in the crack. The integration of this equation from the reference state ($\boldsymbol{E} = 0$, $\boldsymbol{\sigma}_p = 0$ in each crack) provides the link between the macroscopic strain, the aspect ratio and the average of the capillary prestress tensor over the crack

$$\begin{aligned} X - X_0 = (\underline{e}_3 \otimes \underline{e}_3) : \mathbb{T} : \\ \left( (\boldsymbol{E} - \alpha\theta\boldsymbol{\delta}) - \mathbb{C}^{-1} :< \boldsymbol{\sigma}_p > \right), \end{aligned} \tag{19}$$

where $X_0$ denotes the aspect ratio of the crack in the initial configuration.

To evaluate the temperature effects, we consider evolutions of the material made up of cracks with identical radius and aspect ratio randomly distributed in an elastic linear

isotropic solid matrix submited to an isotropic loading defined by $\boldsymbol{\Sigma} = \Sigma\boldsymbol{\delta}$ and $\boldsymbol{E} = E\boldsymbol{\delta}$. As both the material and the loading are isotropic, all the cracks are in the same state (i.e., same capillary prestress and same aspect ratio). As the expressions for $\mathbb{C}_h$ and $\boldsymbol{\Sigma}$ are preserved, the state equation reads when the geometrical non-linearity is taken into account

$$\Sigma = 3k_h\left(E - \alpha\theta\right) + b\sigma_p, \tag{20}$$

where $\sigma_p$ is defined by the second equation 16 when the cracks are unsaturated and $\sigma_p$ is equal to $-p_\ell$ when the cracks are filled only by the liquid phase. The variation of the cracks aspect ratio reads

$$\Delta X = X - X_0 = \frac{9b}{4\pi\varepsilon}(E - \alpha\theta - \frac{\sigma_p}{3k}). \tag{21}$$

Eqs. (16), (20) and (21) describe the behavior of the unsaturated cracked medium submitted to an isotropic loading. The water content, defined here as the ratio of the volume of liquid in the deformed configuration to the volume of the cracks in the reference configuration reads

$$w^{\text{ns}} = \frac{4}{3}\pi\varepsilon\frac{\gamma^3}{a^3X^2p_c^3}. \tag{22}$$

In the saturated regime, Eqs. (20) and (21) are still valid with $\sigma_p = -p_c$ (it is recalled that the gas pressure is naught). The water content is then defined by

$$w^{s} = \frac{4}{3}\pi\varepsilon X. \tag{23}$$

In the sequel, we consider the situation where no macroscopic stress is applied to the material and the gas pressure is taken as reference (i.e., $p_g = 0$). Putting $\Sigma = 0$ into Eq. (21) yields the equation linking the macroscopic isotropic strain $E$ and the temperature $\theta$ to the cracks aspect ratio $X$. Then it is possible to eliminate the aspect ratio of the cracks from the state equations for the isotropic loading under consideration.

The unsaturated evolutions of the system are described by the following dimensionless equations:

$$\overline{p}_c = \frac{p_c}{p_c^\star} = \left(\frac{\gamma(\theta)}{\gamma_0}\right)^{\frac{3}{2}}\sqrt{\frac{-1}{e(1+e)^3}}, \tag{24}$$

with

$$p_c^\star = \sqrt{\frac{b\gamma_0^3}{k_h a^3 X_0^3 n_0}}, \tag{25}$$

and

$$e = \frac{E - \alpha\theta}{3n_0}. \tag{26}$$

In the unsaturated regime, the normalized water content reads

$$\overline{w}^{\mathrm{ns}} = \frac{w^{\mathrm{ns}}}{n_0} = \left(\frac{\gamma(\theta)}{\gamma_0}\right)^{-\frac{3}{2}} (-e)^{\frac{3}{2}}(1+e)^{\frac{5}{2}}. \tag{27}$$

In Eqs. (24) and (27) $n_0$ denotes the porosity in the undeformed configuration. As the closure of the cracks is not consider in this paper, $e$ must belong to the set $[-1, 0]$.

In the saturated regime the cracked media obeys the following state equations:

$$p_c = -\frac{3k_h n_0}{b} e \quad \text{and} \quad \overline{w}^{\mathrm{s}} = 1 + e. \tag{28}$$

Therefore, it appears that taking into account the coupling between the deformation of the pores and the capillary forces modifies the way the capillary pressure and the water content depend on the surface tension in the unsaturated regime. In the framework of the linear model, a temperature change induces a vertical dilatation of the water content–capillary pressure curve proportional to the ratio $\gamma_0/\gamma(\theta)$ whereas temperature changes induce both vertical and horizontal dilatation of the water content–capillary pressure curve when the capillary forces are evaluated on the deformed configuration. Moreover, the intensity of this dilatation does not depend linearly on the ratio $\gamma_0/\gamma(\theta)$ (see Eqs. (24) and (27)). In the saturated regime, the water content–capillary pressure relation ship does not depend on the temperature (see Eqs. (28)).

The predictions of the nonlinear model are depicted in Fig. 5.

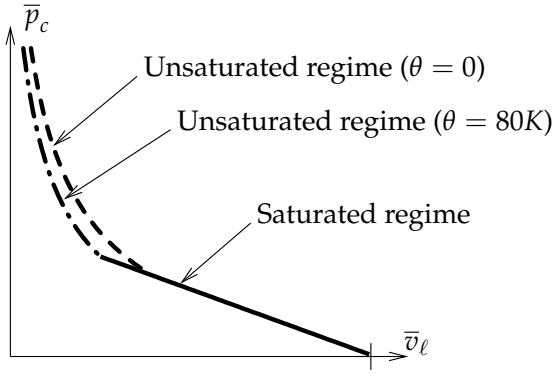


*Fig. 5.* The dimensionless capillary pressure as a function of the dimensionless water content of a free stress unsaturated medium

To compute the data represented in Fig. 5, it was assumed that $\gamma(80K)/\gamma_0 = 0.75$, which corresponds roughly to the ratio of water surface tension at $100C$ over water surface tension at $20C$.

## 5. CONCLUSIONS

Estimates of the temperature effects on the water content-capillary pressure relationship have been proposed within the framework of a micromechanical approach to the behavior of unsaturated porous media. Two different phenomena have been considered: the temperature variations of surface tensions and the thermal dilatation of the solid phase. State law accounting for these two effects have been built when the solid phase in rigid and when the solid phase behaves elastically. Furthermore, it has been shown that taking into account the coupling between the deformation of the porous space and the capillary effects can radically modify the prediction of the temperature influence on the capillary curve.

Of course, some others phenomena like physico-chemical coupling between the solid and the fluid phases cannot be neglected to model the influence of temperature on the behavior of such materials as fine soils at high suctions [1]. Then, we intend to develop micromechanical models accounting for these phenomena in a forthcoming work.

## DECLARATION OF COMPETING INTEREST

The authors declare that they have no known competing financial interests or personal relationships that could have appeared to influence the work reported in this paper.

## ACKNOWLEDGMENTS

This research is funded by Ministry of Education and Training under grand number B2023-XDA-03.

## REFERENCES

[1] E. Romero, A. Gens, and A. Lloret. Temperature effects on the hydraulic behavior of an unsaturated clay. *Geotechnical and Geological Engineering*, **19**, (3/4), (2001), pp. 311–332. https://doi.org/10.1023/a:1013133809333.

[2] P. W. Atkins. *Physical chemistry*. Oxford University Press, (1998).

[3] M. Yekta-Fard and A. B. Ponter. The influences of vapor environment and temperature on the contact angle-drop size relationship. *Journal of Colloid and Interface Science*, **126**, (1), (1988), pp. 134–140. https://doi.org/10.1016/0021-9797(88)90107-5.

[4] X. Chateau and L. Dormieux. Micromechanics of saturated and unsaturated porous media. *International Journal for Numerical and Analytical Methods in Geomechanics*, **26**, (8), (2002), pp. 831–844. https://doi.org/10.1002/nag.227.

[5] F. A. L. Dullien. *Porous media: fluid transport and pore structure*. San Diego: Academic Press, 2nd edition, (1992).

[6] X. Chateau, L. Dormieux, and Y. Xu. Évaluation de l'influence des changements de géométrie sur les déformations de séchage d'un milieu poreux fissuré. *Comptes Rendus Mécanique*, **331**, (2003), pp. 679–686. https://doi.org/10.1016/s1631-0721(03)00146-3.
[7] L. Dormieux, D. Kondo, and F.-J. Ulm. *Microporomechanics*. Wiley, (2006). https://doi.org/10.1002/0470032006.
[8] B. Budiansky and R. J. O'connell. Elastic moduli of a cracked solid. *International Journal of Solids and Structures*, **12**, (2), (1976), pp. 81–97. https://doi.org/10.1016/0020-7683(76)90044-5.
[9] O. Coussy. *Mechanics of porous continua*. John Wiley & Sons, New York, NY, (1995).
[10] X. Chateau, P. Moucheront, and O. Pitois. Micromechanics of unsaturated granular media. *Journal of Engineering Mechanics*, **128**, (8), (2002), pp. 856–863. https://doi.org/10.1061/(asce)0733-9399(2002)128:8(856).
[11] B. V. Tran. *Approche micromécanique du comportement d'un matériau fissuré non saturé*. PhD thesis, Université Paris-Est, (2010).